A framework for developing high-resolution multi-model climate projections: 21st century scenarios for the UK

Jean-Philippe Vidal

HR Wallingford, Howbery Park, Wallingford, Oxfordshire, OX10 8BA, United Kingdom

Tel: +44 (0)1491 822338

Fax: +44 (0)1491 826352

Email: jpv@hrwallingford.co.uk

Steven Wade

HR Wallingford

Abstract

This paper proposes a simple and efficient framework for building consistent climate projections from an ensemble of Global Circulation Models (GCMs) at the local scale required for impact studies. The proposed method relies on a fine-scale gridded baseline climatology and consists of the following steps: (1) building appropriate precipitation and temperature time series from land areas covered by GCM sea cells; (2) correction of GCM outputs inherent biases through “quantile-based mapping”; and (3) disaggregation of bias-corrected outputs with monthly spatial anomalies between GCM-specific and observed spatial scales. The overall framework is applied to derive 21st century seasonal climate projections and interannual variability for the UK based on an ensemble of 6 GCMs run under two different emissions scenarios. Results show a large dispersion of changes within the multi-GCM ensemble, along with a good comparison between scenarios from individual ensemble members and from previous UK and European studies using dynamically downscaled outputs from corresponding GCMs. The framework presented in this paper provides appropriate outputs to take account of the uncertainty in global model configuration within impacts studies that are influencing current decisions on major investments in flood risk management and water resources.

Keywords

Climate change - Multi-model projections – Framework - UK

1. Introduction

Evidence from observed trends in climate variables point towards an intensification in the global hydrological cycle (Huntington, 2006), but large uncertainties remain,at the regional and local scales that are most relevant for climate change impacts studies. Future climate scenarios for precipitation and temperature are usually derived from General Circulation Models (GCMs) projections for given time slices, and are subject to considerable uncertainty arising from various sources listed by Giorgi (2005).

The "cascade of uncertainties" leading to regional scenarios as described by Jones (2000) and New and Hulme (2000) includes the uncertainty in natural forcing in terms of greenhouse gas emissions, the uncertainty in global model configuration, and the uncertainty resulting from the downscaling step. In addition of these uncertainties are those related to specific impact models, for example the rainfall-runoff models used for water resources impact studies (see for example Wilby and Harris, 2006).

The uncertainty in global model configuration has long been recognised as one of the most important part of the overall uncertainty, especially when considering the first decades of the 21st century when the different emissions scenarios do not lead to dramatically different climate responses. Many studies thus recommend the use of an ensemble GCM outputs whose scatter could be taken as a measure of GCM uncertainties (see for example McAveney et al., 2001; Benestad, 2004).

Developing multi-GCM ensembles at the global and regional scale requires consideration of the different strengths and weaknesses displayed by individual GCMs. To this aim, Giorgi and Mearns (2002) proposed the Reliability Average Ensemble (REA) method where GCM raw projections are assigned weights derived from a performance criterion, which reflects the ability to reproduce the present-day climate, and a convergence criterion, defined as the deviation of the individual projection of change with respect to the central tendency of the ensemble. Min et al. (2004) used weights based on based on skill scores proposed by Taylor (2001). Tebaldi et al. (2005) extended the REA approach by using a Bayesian approach and defining a formal statistical model for deriving probabilities from an ensemble of projections. The above studies and more recent ones using similar Bayesian approaches (see for example Furrer et al., 2006; Greene et al., 2006) provided multi-model climate projections either for large sub-continental regions or at a grid scale comparable to the ones from individual GCMs.

In parallel, and in order to get projected scenarios at the scale required for impact studies, many different downscaling techniques have been developed over the last decade. Two main approaches can be identified: the nesting of high-resolution regional climate models (RCMs) in GCMs (dynamical downscaling) and the statistical representation of desired fields from the coarse resolution GCM data (statistical downscaling). As dynamical downscaling is very computationally expensive, only a few experiments involved a RCM driven by a set of different GCMs (Räisänen et al., 2004). Similarly, few large experiments involving statistical downscaling from multi-GCMs

ensemble have been conducted. Indeed, the calibration of this kind of statistical models is relatively time consuming (Prudhomme, 2005).

Building on these limitations of fine-scale multi-model ensemble experiments, this article proposes a framework to develop high-resolution multi-model scenarios which integrate empirical downscaling techniques. This framework is applied to the United Kingdom to derive 21st century climate scenarios at a 5km grid scale. Section 2 presents the data used in this study, and Section 3 describes the methods employed to obtain multi-model fine-scale climate scenarios. The different steps of the data processing framework are assessed in Section 4 for the baseline period. Projected seasonal mean changes for three thirty-year periods of the 21st century are presented and compared with recent European or UK studies in Section 5, and Section 6 shows results on interannual variability for present and future climate.

2. Data

Water resources are dependent upon two main primary variables, which are precipitation and temperature (due to its influence of potential evapotranspiration). Together with catchment properties, the monthly pattern of these two variables controls the seasonal pattern of river flows and groundwater recharge. Consequently, climate scenarios developed in this paper focus only on precipitation and temperature variables.

The baseline reference data for precipitation and temperature were extracted from a gridded data set elaborated by the Met Office (Perry and Hollis, 2005). This observed

data set includes monthly time series for precipitation and temperature for the 1961-1990 period (hereafter referred to as the baseline period) over a 5 km grid covering the United Kingdom. Precipitation and temperature outputs from 6 Global Circulation Models (GCMs) were extracted from the IPCC-DDC website[1] (see Table 1). The GCM runs considered in this study are part of the panel used to produce the Third Assessment Report (TAR) of the Intergovernmental Panel on Climate Change (IPCC, 2001) and cover both A2 and B2 emissions scenarios (Nakicenovic et al., 2000). In this study, we considered three thirty-year time slices centered around the 2020s, the 2050s, and the 2080s.

3. Description of the data processing framework

3.1. Land mask management

To study the impact of climate change on land surface processes, only GCM outputs for land cells should be considered, as rainfall and more particularly temperature patterns are influenced by the nature of the underlying surface. As the different islands composing the UK have complex coastlines, many parts of the country are not within the land mask of one or more GCMs from the set described in Table 1. The process of deriving "land" values is crucial in order to obtain realistic values for some parts of the UK, for example North-East England values as computed by HadCM3. The commonly used approach, used for example in the GCM data archive for UK accompanying the SDSM tool (Wilby et al., 2002), is to take the average values of adjacent cells (Wilby and Dawson, 2004).

[1] http.//ipcc-ddc.cru.uea.ac.uk

The procedure followed here to derive realistic values for a particular sea cell covering land includes four main steps: (1) identify land cells among the nine surrounding cells; (2) apply the two-sided Kolmogorov-Smirnov test (Massey, 1951) to compare monthly distributions of cell-averaged observed data for the sea cell and for each identified surrounding land cell. The observed data have here been taken from the gridded data set derived by Perry and Hollis (2005); (3) Derivation of monthly weights for each surrounding land cell, taken as one minus the corresponding test statistic; (4) Calculation of appropriate 'land values' for the sea cell based on the weighted average of surrounding GCM-derived land cell values.

This procedure has been used for both precipitation and temperature data. It allows taking account of the actual similarity between distributions for the baseline period and does not rely only on closeness or other empirical and cell-specific criteria to define GCM-derived "land" values for sea cells.

3.2. Bias correction

GCM outputs suffer also from biases or systematic errors due to an imperfect model description of the underlying physical processes. A bias-correction scheme based on a "quantile-based mapping" has been adapted from the approach described by Wood et al. (2002, 2004). The principle is to condition the values produced by the GCM for the target period on the correspondence between the observed and control baseline climatologies.

At the GCM grid scale, theoretical statistical distributions are fitted to the cell-averaged observed values for each month, taken from the 5 km gridded data set. A similar fitting is applied to the GCM control run time series. For each month, rainfall and temperature time series are fitted respectively to gamma and normal distributions. These choices have been made accordingly to recent water resources studies (Prudhomme et al., 2005) and verified by computing chi square hypothesis tests which results are shown for each GCM in

Figure 1 for precipitation (lower panels) and temperature (upper panels).

Figure 1 shows that the hypothesis of a gamma distribution for precipitation is verified in most cases for the control runs but not for some specific combinations of month and GCM, for example January and August for HadCM3, and October for ECHAM4. Similarly, the test for a normal distribution for control run temperature only fails for some specific cases, like March for HadCM3, September for GFDL-30, April and May for ECHAM4, and April for CGCM2. Moreover, both tests performed generally better on observed data. In the following, we consequently assumed that the time series actually followed the theoretical distributions. It has to be noted that the spatial resolution over the UK, evaluated in terms of cells covering some UK land, varies considerably from one GCM to another, going from 15 cells for ECHAM4 to only 4 for CSSR/NIES (see Table 1).

Considering a projected value for one month from a GCM-derived time series above a specific cell, it is attributed a probability P in the theoretical distribution for the control run. The value corresponding to the probability P is then extracted from the distribution

for the observed time series for the same month and the same cell. The new value is taken as the bias-corrected value. This process, illustrated in
Figure 2, is repeated for all values in GCM time series. It thus constitutes a step forward the commonly used monthly factors method.

3.3. Spatial disaggregation

The downscaling approach used here requires a fine-scale gridded monthly time series for total precipitation and mean temperature. Once again, the 5 km grid data set derived by Perry and Hollis (2005) was used here. For each GCM, cell-averaged observed monthly means for precipitation and temperature for the baseline period have been computed at the GCM grid scale and then interpolated back bi-linearly to the finer grid scale. Precipitation monthly anomalies are computed at the finer grid scale by dividing the observed monthly means by the resulting monthly means. Temperature monthly anomalies have similarly been computed by subtracting the resulting monthly means for temperature from the observed monthly means. The outputs are GCM-specific 5 km grid of spatial anomalies for each month of the year, showing the difference between the finer grid and the corresponding GCM grid.

Spatial fields from each GCM are first bias-corrected thanks to the procedure detailed above. Monthly time series are then bi-linearly interpolated to the finer grid scale, and finally multiplied by (for precipitation) or summed with (for temperature) monthly spatial anomalies to get a finer spatial pattern. This approach makes use of both aspects of GCM outputs, which can be interpreted as point or areal quantity, as pointed out by

Skelly and Henderson-Sellers (1996) and Osborn (1997). The spatial disaggregation method used here implies that the small-scale variability depends only on the synoptic scale (Hewitson and Crane, 2006), and assumes that the spatial variation within a grid square will remain unchanged in the future.

Widmann et al. (2003) used a similar approach called “local scaling” to demonstrate the potential of GCM precipitation as a predictor for precipitation downscaling in the north-western United States. This approach was then used by Salathé (2003) to simulate streamflow in a rainshadow river basin and compared with more sophisticated techniques. This simple downscaling technique has also been used for the elaboration of climate change scenarios for the UK (Hulme and Jenkins, 1998).

The bias-correction and spatial disaggregation have been used by Wood et al. (2004) to downscale outputs from the PCM (Parallel Climate Model) GCM (resolution ~2.8 degrees) to a 0.125 degrees resolution grid corresponding to an observed climatology for the US Pacific Nortwest domain. They compared three downscaling approaches through a twenty-year retrospective analysis: linear interpolation, spatial disaggregation and bias-corrected spatial disaggregation. The corresponding meteorological outputs were then used to drive a macroscale hydrological model. Wood et al. (2004) conclude that the later approach, which is used in the present study, is successful in reproducing observed hydrology at the monthly scale.

4. Method assessment

The impact of the overall method on GCM data for the baseline period can be assessed by plotting Taylor diagrams (Taylor, 2001) with reference to the observed climatology. This type of diagram has been widely used for global climate model evaluation and comparison (see for example Covey, 2003) and is here applied to assess different stages of refinement of GCM outputs.

The Taylor diagrams for rainfall and temperature twelve months cycle averaged over the UK 5 km grid cells are shown respectively in Figure 3 and Figure 4. In each diagram, the radial coordinate gives the magnitude of total standard deviation of the data considered, and the angular coordinate gives the correlation with the corresponding observed field. It follows that the distance between the reference point and any model's point is proportional to the root mean square model error. For each variable, a model score has be computed to quantify the skill reached after each processing step by using the following formula proposed by Taylor (2001):

$$S = \frac{4\left(1+R\right)}{\left(\hat{\sigma}_f + 1/\hat{\sigma}_f\right)^2\left(1+R_0\right)} \qquad (1)$$

where $\hat{\sigma}_f$ is the normalized standard deviation of the GCM field, and R the correlation coefficient between the GCM-derived and observed fields. R_0 represents the maximum correlation attainable and is here equal to 1.

The effects of each processing step on precipitation fields can be assessed by examining Figure 3. It first shows that these effects are roughly similar for all GCMs considered.

The land management step reduces the variance by considering only annual cycles related to land cells which show different climatological patterns from sea cells. The bias correction step increases slightly the correlation and particularly brings the variance values much closer to the one for the observed annual cycle, highlighting the importance of this step. As can be expected, interpolation increases the correlation and reduces slightly the variance. Spatial disaggregation finalizes the process by assuring the equality of observed and GCM-derived precipitation annual cycles. As a consequence of the bias correction and spatial disaggregation steps, this property is also verified for every 5 km grid cell.

Figure 4 presents a slightly different picture for temperature annual cycles. It first has to be noted that the initial discrepancies in variance are far less than for precipitation, with specific GCMs showing either higher or lower variance than the observed one. Correlation between raw GCM and observed climatologies is also higher than for precipitation. These two comments confirm previous general comparisons made at the global scale that GCMs raw computation of temperature is far more reliable than that of precipitation (McAveney et al., 2001). For most of the models, the land management step tends to reduce the error in variance. The bias correction dramatically increases the correlation and closely gathers statistics from all GCMs. As temperature is at a coarse scale less spatially variable than precipitation, the improvement due to interpolation is here very limited. The addition of spatial anomalies allows taking account of local features like elevation to reach the agreement between observed and GCM-derived temperature annual cycles at the 5 km grid scale.

Furthermore, the two-sided Kolmogorov-Smirnov test has been used to compare for each 5 km grid cell the statistical distributions of observed and ensemble GCM-derived baseline precipitation and temperature. The hypothesis of common distributions is verified at the 95% confidence level for each month for more than 96% of the UK for precipitation, and for more than 99% for temperature.

5. Seasonal changes for the UK

For a given time slice and a given emissions scenario, projections from the six different GCMs are considered in the analysis as equally likely representations of future climate. This hypothesis takes root in the application of the bias-correction scheme described in section 3.2. Consequently, ensemble monthly statistics (monthly mean and standard deviation) are here computed directly from 6 x 30 years time series. The next sections highlight some of the results. In the following, seasons are defined as three-month periods: DJF (winter), MAM (spring), JJA (summer), and SON (autumn).

5.1. Precipitation

Figure 5 shows the percent changes in precipitation averaged over the UK, as computed by each of the ensemble members along with the ensemble mean. These changes are computed for thirty-years periods centred on the 2020s, 2050s, and 2080s with respect to the observed baseline climate. Results from the ensemble means show an increase in precipitation in winter, larger under the A2 scenario than under the B2 scenario. This change in precipitation becomes larger towards the end of the century, reaching +35%

in the 2080s according to the ensemble mean. The intra-ensemble variability also increases with time, with some GCMs showing an increase of 60 to 80 percent. The overall pattern for spring is broadly similar from winter, but with a smaller magnitude of changes. It also has to be noted that changes under the B2 scenario are slightly larger than under the A2 scenario. In summer, precipitation decreases linearly with time, up to -20% in the 2080s under the A2 scenario. As for winter, changes are smaller under the B2 scenario, and intra-ensemble variability increases with time. The pattern for autumn is quite different, showing a relatively stable increase of 5 to 9% for all three future periods compared to 1961-1990.

Figure 6 presents the spatial pattern of the ensemble mean change in seasonal precipitation for the A2 emissions scenario. The overall pattern for winter is a homogeneous increase in precipitation over the UK. Spring precipitation is also expected to increase, with larger changes (more than +25% in the 2080s) in the North-West of the country, compared to a relatively small +5% in South-East England. In summer, projected precipitations are expected to be far smaller than for the baseline period, with larger changes (up to more than 30% in the 2080s) in the South-East, to be compared with less than 10% decrease in North-West Scotland. The overall pattern for the autumn is very similar to the one for spring, but with slightly smaller changes. When looking towards the end of the century, differences between the north and south of the UK become more and more prominent, even for autumn when the UK-averaged change is relatively stable (see Figure 5). The spatial patterns of changes under the B2 scenario are not shown for brevity, but it is important to note that the north-south differences

computed under the A2 scenario are largely reduced, particularly in spring when both scenarios yet exhibit similar UK-averaged changes.

5.2. Temperature

The percent changes in temperature averaged over the UK, as given by each ensemble members and the ensemble mean, are shown in Figure 7. The overall pattern for the UK is far simpler than for precipitation, as it follows the global warming pattern computed by GCMs. Accordingly, the rate of warming is smaller under the B2 scenario. The projected ensemble means reach +4°C in summer for the 2080s under the A2 scenario, but individual GCMs show an increase of up to 6.5°C. Indeed, the intra-ensemble variability increases significantly with time for all seasons.

Figure 8 presents the spatial pattern of the ensemble-averaged change in seasonal temperature. In winter, the warming is expected to be larger in the South-East England than in the Scottish Highlands. Simulations for summer and autumn show a very similar spatial pattern, with an increase of more than 4.4°C in summer for South-Central England. Changes for spring precipitation are on the contrary very homogeneous over the UK. As for precipitation, the north-south differences are reduced under the B2 scenario, especially for summer temperatures (not shown).

5.3. Comparison with results from previous UK and European studies

Several studies recently focused on climate changes over UK and Europe for the 2080s, using dynamical downscaling approaches. The following paragraphs propose some qualitative comparisons between results from these studies and the ones described in the two previous sections. For clarity purpose, results from each ensemble member will be referred as the name of the corresponding GCM followed by "-em", and ensemble scenarios will be referred to as GCME.

First, maps shown in Figure 6 and Figure 8 have been drawn specifically for comparison with similar maps produced for the UKCIP02 scenarios (Hulme et al., 2002, p. 31 and 35). These scenarios are based on runs from the Hadley Centre regional model HadRM3 driven by HadCM3 for the 2080s under the A2 emissions scenario (called Medium-High Emissions scenario). They form the basis of the UK Climate Impact Programme scenarios (UKCIP02) that are used widely for regional and local climate change impacts studies in England and Wales, Scotland and Northern Ireland. Changes for other time-slices and emissions scenarios were derived using simple scaling factors. Consequently, the following comparisons will focus on the 2080s and A2 scenario to ensure consistency with the original GCM outputs. However, UK-averaged results for both A2 and B2 emissions scenarios and for the three time-slices are shown for comparison in Figure 5 for precipitation and Figure 7 for temperature.

The UKCIP02 precipitation scenario for winter shows very spatially variable changes, ranging from 0 to 30%, when ensemble-mean projections show larger and particularly homogenous changes. On the other hand, north-south differences mentioned in Section 5.1 for other seasons were well reproduced by this UKCIP02 scenario in term of the

amplitude of spatial variability, but the magnitudes of changes are very different from the ensemble means. Indeed, these UKCIP02 changes reflect those computed by the driving HadCM3. In Figure 5, long arrows indicate changes computed from HadCM3 ensemble member outputs (HadCM3-em). Compared to the ensemble result, HadCM3-em –as well as HadRM3 through UKCIP02– shows smaller precipitation increase (or even decrease) in winter, spring and autumn, and a larger precipitation decrease in summer. Indeed, Hulme et al. (2002) have already pointed out that HadCM3 (and consequently UKCIP02 scenarios) shows the driest summer projections among the GCMs considered here.

UKCIP02 temperature scenario for winter and summer show more spatially variable changes than projections from GCME. According to the ensemble results, Scotland should warm less than projected by UKCIP02 scenario, leading to a smaller UK-averaged warming. This pattern is in agreement with the results from HadCM3-em, especially for winter and summer (see Figure 7). The homogeneous changes of 2.5-3°C projected by UKCIP02 and GCME for spring agree well, but UKCIP02 autumn changes are larger than the ones projected GCME, which cannot be explained by HadCM3-em.

In the PRUDENCE[2] project, a range of global and regional climate models were used as a common framework to produce climate change projection s for Europe and to advance the uncertainty analysis of regional climate change (Christensen et al., 2002).

[2] Prediction of Regional scenarios and Uncertainties for Defining EuropeaN Climate change risks and Effects: http://prudence.dmi.dk/

Giorgi et al. (2004) used the regional climate model RegCM (Pal et al., 2000) driven by the HadAM3H version of the Hadley Centre GCM and averaged results for the 2080s under the A2 and B2 scenarios over different European sub-regions. Precipitation and temperature changes obtained for the British Isles are broadly similar to the ones obtained in the present study by HadCM3-em (indicated by long arrows in Figure 5), and thus suffer from the same biases as in UKCIP02 scenario.

Rowell (2006) computed spatially averaged changes for the British Isles for the 2080s based on 9 different RCMs driven once again by HadAM3H under the A2 emissions scenario. Results show a dispersion of precipitation changes in winter and summer spanning approximately from the HadCM3-em value to a much smaller change. For the intermediate seasons, results indicate either positive or negative precipitation changes, whereas HadCM3-em shows a small but noticeable increase. Comparison for temperature results is more clear-cut, as the multi-RCMs results are regrouped within a 0.5 to 1°C width range centred on the HadCM3-em value, for all seasons but autumn, when changes are closer to results from GCME. It has to be noted that this autumn pattern can also be found in RegCM simulations described by Giorgi et al. (2004).

Déqué et al. (2005) used nine regional climate models all driven by HadAM3H to investigate the response of the A2 emissions forcings for the 2080s in Europe. The winter and summer temperature response over the UK computed as the mean of the nine RCMs simulations response is once again lower than results from GCME, as is the response from HadCM3-em.

Each study referenced above produced scenarios based on projections from a single GCM, which was one or another version of the Hadley Centre GCM. This brief review points to the fact that UK-averaged changes from all these studies, along with the UKCIP02 main spatial features, are very close to results obtained by the HadCM3-em, at least for extreme seasons. Furthermore, Figure 5 and Figure 7 show that projections from this ensemble member differ significantly from the ensemble mean projection.

Räisänen et al. (2004) compared winter and summer results for Europe computed by the Swedish Rossby Centre regional model (RCAO, Doscher et al., 2002) driven by two different GCMs (HadAM3H and ECHAM4/OPYC3) under both A2 and B2 scenarios for the 2080s. One of the most interesting conclusions in the context of the present study is that the magnitude and the geographical patterns of precipitation and temperature change differ substantially when using different driving GCMs. In Figure 5 and Figure 7, long and short arrows indicate respectively HadCM3-em and ECHAM4/OPYC3-em. These two GCMs individually give very different UK-averaged changes, and temperature changes are spread on both sides of the ensemble mean values. Not surprisingly, when comparing these values with the ones obtained by Räisänen et al. (2004), it can be seen that UK-averaged changes computed with each driving GCM scenario are very close to the corresponding ensemble member values, for both emissions scenarios and for both extreme seasons. It leads to the conclusion that the largest part of uncertainty in UK climate changes is due to the GCM formulation, and not to the downscaling method used. This is supported by Rowell (2006), who found that the uncertainty in the formulation of the RCM has a relatively small impact on the range of possible outcomes of future UK seasonal climate.

It is important to note that projected changes from all the above studies are relative to control simulations, and not to the observed baseline climate. In spite of this difference from the present study, the above comparisons indicate a relatively good agreement on the magnitude of these changes when considering individual ensemble members and their corresponding dynamically downscaled counterparts.

5.4. Comparison with observed trends

The above ensemble predictions can also be compared with observed trends in the UK. Perry (2006) compared the change in mean temperature between the 1961-1990 and 1991-2004 averages for the 5 km grid used in the present study and found an overall warming which is more pronounced for the south-east of the country in all seasons. This spatial pattern agrees well to both previous studies (Jones and Lister, 2004) and to the ensemble predictions shown in Figure 8. Perry (2006) also studied the change in precipitation between 1961 and 2004. The overall trends in winter (overall increase) and in summer (overall decrease, more pronounced in the south) compares well with results presented in Figure 6. For intermediate seasons, the great heterogeneity in the observed trends makes the comparison much more difficult. Moreover, the detailed spatial pattern of trends in Scotland is not really consistent with projected changes, as already shown by Barnett et al. (2006).

6. Interannual variability

We here investigate the interannual variability in the baseline and future time series. This variability and its changes may have substantial consequences compared to the changes in seasonal means only, for example on the frequency of multi-season droughts. The linear trends from each 30-year seasonal time series from individual GCMs were first removed. As pointed out by Giorgi et al. (2004), this step is necessary to filter out the effects of trends within each 30-year period, including the baseline period. The individual GCM and ensemble standard deviation for each run were then computed from these detrended time series. A similar process was applied to observed reference time series. The standard deviation was here used as a measure of temperature interannual variability, and the coefficient of variation was adopted for precipitation, in order to make results independent from the mean.

6.1. Precipitation

Figure 9 shows the precipitation interannual coefficient of variation, for the baseline period (here noted as the 1970s) and for the three future periods considered. The first point worth noting is that the baseline period interannual variability is underestimated for all seasons. Indeed, the spatial variability of this measure is very large within the observed data set, with high values in specific parts of the country, varying from one season to another (not shown). This spatial variability is not reproduced with the approach presented in Section 3 which focused primarily on the fitting of means.

Changes in interannual variability can still be investigated by comparing future scenarios with corresponding control runs. According to results from GCME, the

summer season should be the only one to experience a significant increase in variability for the end of the century. Giorgi et al. (2004) and Rowell (2005) arrived to the same conclusion when using respectively the RegCM RCM driven by HadAM3H and the high resolution GCM HadAM3P. Results from these two studies qualitatively compare well with results from the individual HadCM3 ensemble member, which shows a decrease in winter, a small decrease in spring, a increase in summer larger than the one shown by GCME, and a slight decrease in autumn.

6.2. Temperature

Figure 10 shows the temperature interannual standard deviation, for the baseline period and for the three future periods considered. Contrary to precipitation, the baseline period variability is relatively well reproduced by GCME, with only slight discrepancies in winter and autumn, resulting once again from the spatial variability of this measure in the observed climate (not shown). Predicted changes between GCME control and future scenarios are only noticeable for winter (decrease) and summer (increase). It can be noted that the summer increase predicted by HadCM3-em is far larger than the one from GCME (see arrows in Figure 10). Not surprisingly, this significant and specific pattern has been pointed out by Giorgi et al. (2004) and Rowell (2005) when studying results from Hadley Centre GCMs.

7. Conclusions

This article presented a framework for developing multi-GCMs fine-scale ensemble projections. This three-step framework is easy to implement and not computationally expensive. It thus provides a simple but nevertheless robust approach to combine outputs from different GCMs. Indeed, regional downscaling methods require coupled GCM-RCM experiments which are very computationally expensive and may raise modelling inconsistencies between the two spatial scales. On the other hand, commonly used statistical downscaling methods as SDSM (Wilby et al., 2002) are ideal for detailed local studies but are less practical for national scale impact studies.

The bias correction step performed on each variable allows considering outputs from different GCMs as an equally weighted ensemble. The quantile-based mapping avoids choosing weighting criteria as in the original REA method described by Giorgi and Mearns (2002). The empirical-statistical downscaling method described in Section 3.3 appears to be robust enough to provide consistent spatial patterns, as demonstrated by previous studies (Wood et al., 2002; Salathé, 2003), and more detailed multi-model comparisons between statistical downscaling methods for three catchment case studies are currently under way. Moreover, as shown in Section 15, results from HadCM3-em compare well with the ones from different RCMs driven by the Hadley Centre GCM, showing that the uncertainty in downscaling technique is much smaller than the uncertainty related to global model configuration.

In the UK and a number of other European countries, climate change is being integrated into decision making processes at the national, regional and local scales. The impacts of climate change affect major investment decisions in flood risk management, water

resources planning, spatial planning and implementation of the Water Framework Directive. Therefore, the approach presented in this paper can be used for the integration of uncertainties related to climate change into decision making processes for a wide range of applications (Beven et al., 2006). Indeed, it provides ensemble high resolution future climate monthly time series which can be directly used by impact models to provide regional and catchment scale scenarios.

The uncertainty in the global model structure is considered as the largest one in the process of deriving climate projections for impact studies, and thus requires a particular attention (Prudhomme, 2006, Wilby and Harris, 2006). This uncertainty can be described more accurately as the number of GCMs developed around the world increases. Indeed, more than twenty GCMs are currently considered within the Fourth Assessment Report (AR4) of the IPCC, and this framework can actually be useful both to develop multi-model projections and to estimate the uncertainty on impacts derived from the configuration of the global models.

8. Acknowledgements

This research was supported by a European Commission Marie Curie Research Fellowship and additional research funding from UK Water Industry Research Ltd. and the UK Environment Agency (project CL\04\C).

9. References

Barnett C, Hossell J, Perry M, Procter C, Hughes G. 2006. Patterns of climate change across Scotland: Technical Report. SNIFFER Project CC03, Scotland and Northern Ireland Forum for Environmental Research.

Benestad RE. 2004. Tentative probabilistic temperature scenarios for northern Europe. Tellus A 56: 89-101. DOI: 10.1111/j.1600-0870.2004.00039.x

Beven KJ, Romanowicz RJ, Wade SD, Vidal J-P, Barnett C. 2006. Effect of Climate Change on River Flows and Groundwater Recharge, A Practical Methodology: A Strategy for Evaluating Uncertainty in Assessing the Impacts of Climate Change on Water Resources. UKWIR Report 05/CL/04/6, United Kingdom Water Industry Research.

Christensen JH, Carter TR, Giorgi F. 2002. PRUDENCE employs new methods to assess European climate change. EOS 83: 147.

Covey C, AchutaRao KM, Cubasch U, Jones P, Lambert SJ, Mann ME, Phillips TJ, Taylor KE. 2003. An overview of results from the Coupled Model Intercomparison Project. Global and Planetary Change 37: 103-133. DOI: 10.1016/S0921-8181(02)00193-5

Delworth TL, Stouffer RJ, Dixon KW, Spelman MJ, Knutson TR, Broccoli AJ, Kushner PJ, Wetherald RT. 2002. Review of simulations of climate variability and change with the GFDL R30 coupled climate model. Climate Dynamics 19: 55-574. DOI: 10.1007/s00382-002-0249-5

Déqué M, Jones RG, Wild M, Giorgi F, Christensen JH, Hassell DC, Vidale PL, Rockel B, Jacob D, Kjellström E, de Castro M, Kucharski F, van den Hurk B. 2005.

Global high resolution versus Limited Area Model climate change projections over Europe: quantifying confidence level from PRUDENCE results. Climate Dynamics 25: 653-670. DOI: 10.1007/s00382-005-0052-1

Döscher R, Willén U, Jones C, Rutgersson A, Meier HME, Hansson U, Graham LP. 2002. The development of the coupled regional ocean-atmosphere model RCAO. Boreal Environment Research 7: 183-192.

Emori S, Nozawa T, Abe-Ouchi A, Numaguti A, Kimoto M, Nakajima T. 1999. Coupled ocean-atmosphere model experiments of future climate change with an explicit representation of sulfate aerosol scattering. Journal of the Meteorological Society of Japan 77: 1299-1307.

Flato GM, Boer GJ. 2001. Warming asymmetry in climate change simulations. Geophysical Research Letters 28: 195-198. DOI: 10.1029/2000GL012121

Furrer R, Sain SR, Nychka D, Meehl G. 2006. Multivariate bayesian analysis of atmosphere-ocean General Circulation Models. Environmental and Ecological Statistics, in press.

Giorgi F. 2005. Climate change prediction. Climatic Change 73: 239-265. DOI: 10.1007/s10584-005-6857-4

Giorgi F, Bi X, Pal J. 2004. Mean, interannual variability and trends in a regional climate change experiment over Europe. II: Future climate scenarios (2071-2100). Climate Dynamics 23: 839-858. DOI: 10.1007/s00382-004-0467-0

Giorgi F, Mearns LO. 2002. Calculation of average, uncertainty range, and reliability of regional climate changes from AOGCM simulations via the “Reliability Ensemble Averaging” (REA) method. Journal of Climate 15: 1141-1158. DOI: 10.1175/1520-0442(2002)015<1141:COAURA>2.0.CO;2

Gordon HB, O'Farrell SP. 1997. Transient climate change in the CSIRO coupled model with dynamic sea ice. Monthly Weather Review 125: 875-907. DOI: 10.1175/1520-0493(1997)125<0875:TCCITC>2.0.CO;2

Greene AM, Goddard L, Lall U. 2006. Performance-based multimodel climate change scenarios 1: Low-frequency temperature variations. Journal of Climate, in press.

Hewitson BC, Crane RG. 2006. Consensus between GCM climate change projections with empirical downscaling. International Journal of Climatology 26: 1315-1337. DOI: 10.1002/joc.1314

Huntington TG. 2006. Evidence for intensification of the global water cycle: Review and synthesis. Journal of Hydrology 319: 83-95. DOI: 10.1016/j.jhydrol.2005.07.003

Hulme M, Jenkins GJ. 1998. Climate Change Scenarios for the UK: Scientific Report. UKCIP Technical report 1.

Hulme M, Jenkins GJ, Lu X, Turnpenny JR, Mitchell TD, Jones RJ, Lowe J, Murphy JM, Hassel D, Boorman P, McDonald R, Hill S. 2002. Climate Change Scenarios for the United Kingdom: The UKCIP02 Scientific Report. Tyndall Centre for Climate Change Research, School of Environmental Sciences, University of East Anglia. Norwich, UK.

IPCC. 2001. Climate Change 2001: The Scientific Basis. Contribution of Working Group I to the Third Assessment Report of the Intergovernmental Panel on Climate Change [Houghton JT, Ding Y, Griggs DJ, Noguer M, van der Linden PJ, Dai X, Maskell K, Johnson CA (eds.)]. Cambridge University Press, Cambridge, United Kingdom and New York, NY, USA, 881pp.

Johns TC, Gregory JM, Ingram WJ, Johnson CE, Jones A, Lowe JA, Mitchell JFB, Roberts DL, Sexton DMH, Stevenson DS, Tett SFB, Woodage MJ. 2003. Anthropogenic climate change for 1860 to 2100 simulated with the HadCM3 model under updated emissions scenarios. Climate Dynamics 20: 583-612. DOI: 10.1007/s00382-002-0296-y

Jones RN. 2000. Managing uncertainty in climate change projections – Issues for impacts assessments. Climatic Change 45: 403-419. DOI: 10.1023/A:1005551626280

Jones PD, Lister D. 2004. The development of monthly temperature series for Scotland and Northern Ireland. International Journal of Climatology 24: 569-590. DOI: 10.1002/joc.1017

McAveney BJ, Covey C, Joussaume S, Kattsov V, Kitoh A, Ogana W, Pitman AJ, Weaver AJ, Wood RA, Zhao Z-C. 2001. Model evaluation. In: Climate Change 2001: The Scientific Basis. Contribution of Working Group I to the Third Assessment Report of the Intergovernmental Panel on Climate Change [Houghton, JT, Ding Y, Griggs DJ, Noguer M, van der Linden PJ, Dai X, Maskell K, Johnson CA (eds.)]. Cambridge University Press: Cambridge, United Kingdom and New York, NY, USA, 881p.

Massey FJ. 1951. The Kolmogorov-Smirnov test for goodness of fit. Journal of the American Statistical Association 46: 68-78. DOI: 10.2307/2280095

Min S-K, Park E-H, Kwon W-T. 2004. Future projections of East Asian climate change from multi-AOGCM ensembles of IPCC SRES scenario simulations. Journal of the Meteorological Society of Japan 82: 1187-1211. DOI: 10.2151/jmsj.2004.1187

Nakicenovic N, Swart R (Eds). 2000. Special Report on Emissions Scenarios. Cambridge University Press: Cambridge.

New M, Hulme M. 2000. Representing uncertainty in climate change scenarios: a Monte-Carlo approach. Integrated Assessment 1: 203-213. DOI: 10.1023/A:1019144202120

Osborn TJ. 1997. Areal and point precipitation intensity changes: implications for the application of climate models. Geophysical Research Letters 24: 2829-2832. DOI: 10.1029/97GL02976

Pal JS, Eltahir EAB, Small EE. 2000. Simulation of regional-scale water and energy budgets - Representation of subgrid cloud and precipitation processes within RegCM. Journal of Geophysical Research 105: 29579-29594. DOI: 10.1029/2000JD900415

Perry M. 2006. A spatial analysis of trends in the UK climate since 1914 using gridded datasets. Climate Memorandum No 21, National Climate Information Centre, Met Office.

Perry M, Hollis D. 2005. The generation of monthly gridded datasets for a range of climatic variables over the UK. International Journal of Climatology 25: 1041-1054. DOI: 10.1002/joc.1161

Prudhomme C. 2006. GCM and downscaling uncertainty in modelling of current river flow: why is it important for future impacts? In: Climate Variability and Change-Hydrological Impacts (Proceedings of the Fifth FRIEND World Conference). IAHS Red Book Series 308, IAHS Publications: Wallingford.

Prudhomme C, Piper B, Osborn T, Davies H. 2005 Climate change uncertainty in water resource planning. UKWIR Report 05/CL/04/4, United Kingdom Water Industry Research.

Räisänen J, Hansson U, Ullerstig A, Döscher R, Graham L, Jones C, Meier H, Samuelsson P, Willén, U. 2004. European climate in the late twenty-first century: regional simulations with two driving global models and two forcing scenarios. Climate Dynamics 22: 13-31. DOI: 10.1007/s00382-003-0365-x

Rowell DP. 2005. A scenario of European climate change for the late twenty-first century: seasonal means and interannual variability. Climate Dynamics 25: 837-849. DOI: 10.1007/s00382-005-0068-6

Rowell DP. 2006. A demonstration of the uncertainty in projections of UK climate change resulting from regional model formulation. Climatic Change, in press.

Salathé EP. 2003. Comparison of various precipitation downscaling methods for the simulation of streamflow in a rainshadow river basin. International Journal of Climatology. 13: 887-901. DOI: 10.1002/joc.922

Skelly WC, Henderson-Sellers A. 1996. Grid box or grid point: what type of data do GCMs deliver to climate impacts researchers? International Journal of Climatology 16: 1079-1086.

Stendel M, Schmith T, Roeckner E, Cubash U. 2002. The climate of the 21st century: Transient simulations with a coupled atmosphere-ocean general circulation model. Revised version. Report 02-1. Danish Meteorological Institute.

Taylor KE. 2001. Summarizing multiple aspects of model performance in a single diagram. Journal of Geophysical Research 106: 7183–7192. DOI: 10.1029/2000JD900719

Tebaldi C, Smith RL, Nychka D, Mearns LO. 2005. Quantifying Uncertainty in Projections of Regional Climate Change: A Bayesian Approach to the Analysis of Multimodel Ensembles. Journal of Climate 18: 1524-1540. DOI: 10.1175/JCLI3363.1

Widmann M, Bretherton CS, Salathé EP. 2003. Statistical precipitation downscaling over the Nothwestern United States using numerically simulated precipitation as a predictor. Journal of Climate 16: 799-816. DOI: 10.1175/1520-0442(2003)016<0799:SPDOTN>2.0.CO;2

Wilby RL, Dawson CW. 2004. Using SDSM Version 3.1 – A Decision Support Tool for the Assessment of Regional Climate Change Impacts. User manual. Available from http://www-staff.lboro.ac.uk/~cocwd/SDSM/

Wilby RL, Dawson CW, Barrow EM. 2002. SDSM – A decision support tool for the assessment of regional climate change impacts. Environmental Modelling and Software 17: 145-157. DOI: 10.1016/S1364-8152(01)00060-3

Wilby RL, Harris I. 2006. A framework for assessing uncertainties in climate change impacts: Low-flow scenarios for the River Thames, UK. Water Resources Research 42: W02419. DOI: 10.1029/2005WR004065

Wood AW, Maurer E, Kumar A, Lettenmaier DP. 2002. Long-range experimental hydrologic forecasting for the eastern United States. Journal of Geophysical Research 107: D20. DOI: 10.1029/2001JD000659

Wood AW, Leung LR, Sridhar V, Lettenmaier DP. 2004. Hydrologic implications of dynamical and statistical approaches to downscaling climate model outputs. Climatic Change 62: 189-216. DOI: 10.1023/B:CLIM.0000013685.99609.9e

Table 1: Summary of GCMs used. TCR (Transient Climate response) shows the increase in global temperature as response to a standardized 1%/year increase in CO_2 at the time of CO_2 doubling (IPCC, 2001). Last column shows the number of cells covering some UK land. In brackets is given the number of land cells for the UK.

Model	Research Centre	Reference	TCR (°C)	Number of cells
HadCM3	Hadley Centre for Climate Prediction and Research, UK	(Johns et al., 2003)	2.0	13 (5)
CGCM2	Canadian Center for Climate Modelling and Analysis, Canada	(Flato and Boer, 2001)	1.92	11 (6)
CSIRO-mk2	Commonwealth Scientific and Industrial Research Organisation, Australia	(Gordon and O'Farrell, 1997)	2.0	9 (4)
GFDL-R30	Geophysical Fluid Dynamics Laboratory, USA	(Delworth et al., 2002)	1.96	15 (7)
CCSR/NIES	Center for Climate System Research /	(Emori et al., 1999)	3.1	4 (1)

	National Institute for Environmental Studies, Japan			
ECHAM4/OPYC3	Max Planck Institute für Meteorologie, Germany	(Stendel et al., 2002)	1.4	16 (7)

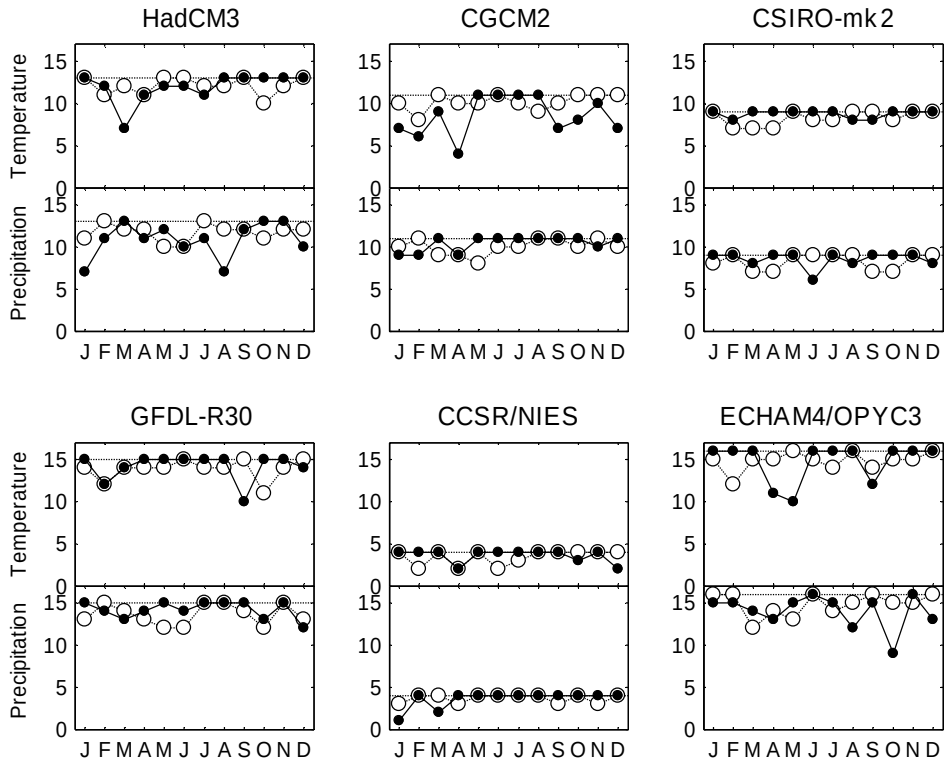

Figure 1. Number of GCM cells above UK land with monthly precipitation following a gamma distribution (lower panels) and with monthly temperature following a normal distribution (upper panels) according to the chi-square test. White circles denote observed data spatially averaged to the GCM grid and black filled circles represent GCM control run outputs. Dashed lines show the total number of cells above UK land as given in Table 1.

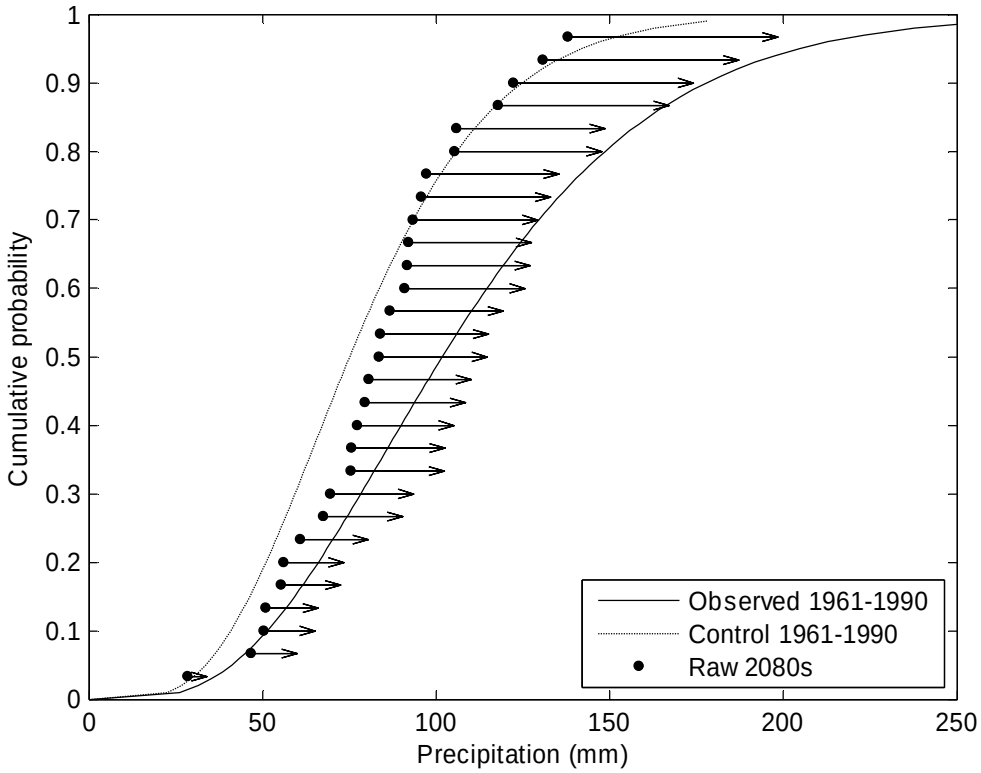

Figure 2. Illustration of the bias correction process on January precipitation amounts computed by HadCM3 above Wales for the 2080s. Solid and dotted lines represent gamma distributions fitted respectively to cell-averaged observed data and GCM-derived control data. Black circles denote raw values projected by HadCM3 for the 2080s, and arrow ends show corresponding bias-corrected values.

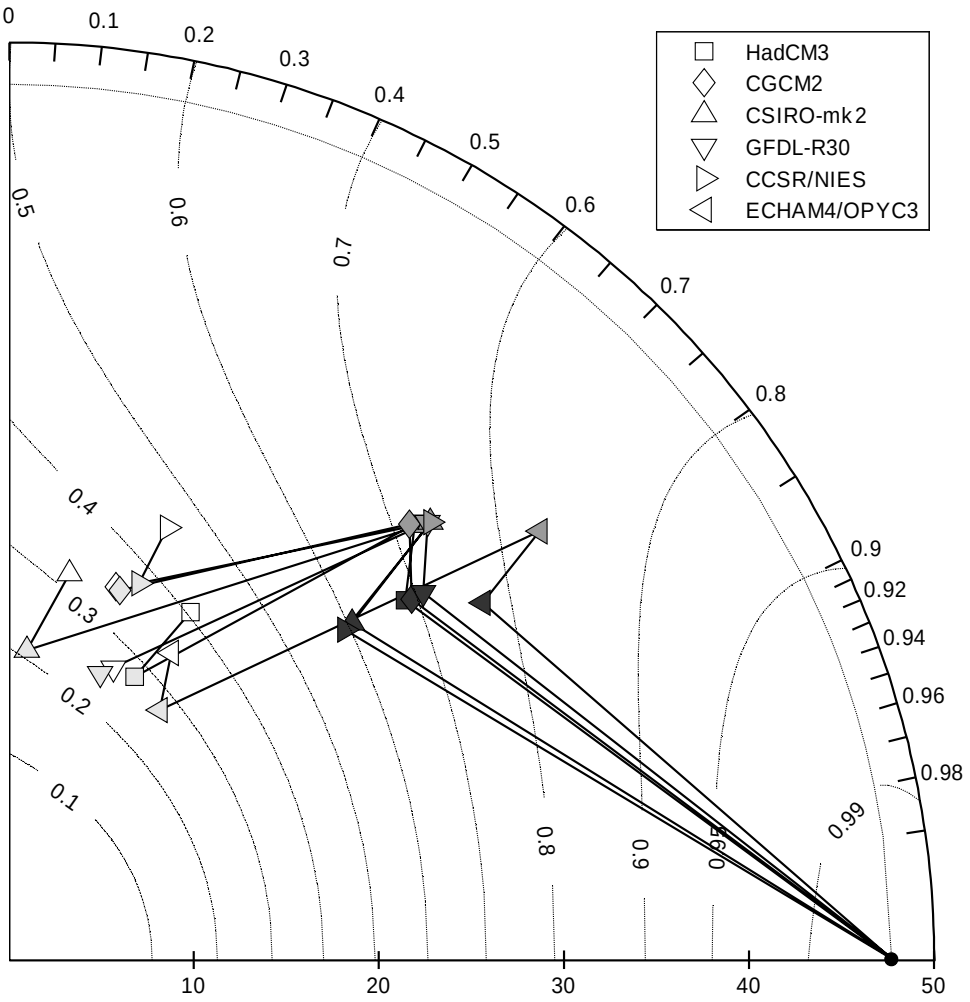

Figure 3. Taylor diagram for normalized pattern statistics describing baseline period twelve months annual cycles of precipitation at the 5 km grid scale. White markers correspond to raw GCM data. Light, medium and dark grey indicate respectively data after land mask management, bias correction, and interpolation. The black circle corresponds both to observed climatology and spatially disaggregated climatologies for each GCM. The dashed circular line corresponds to the reference standard deviation in the annual cycle. Dotted contour lines represent the skill score as given by equation (1). See text for interpretation.

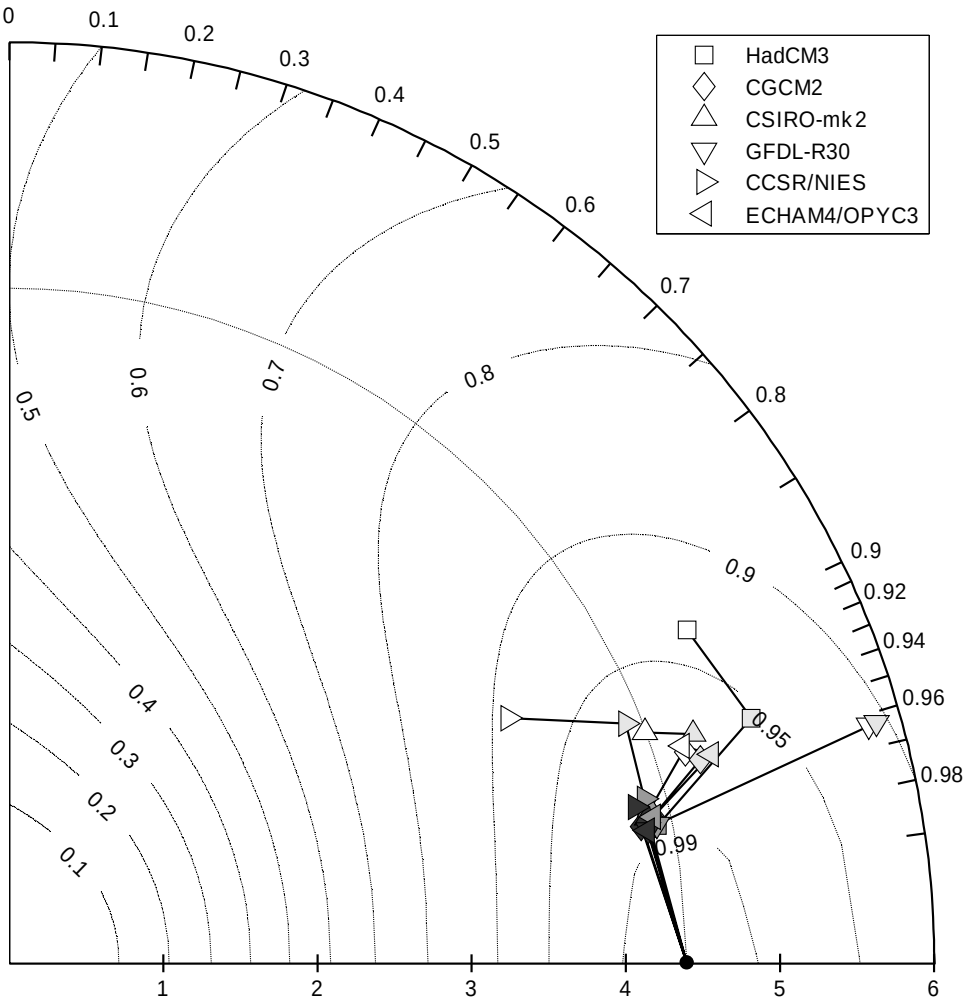

Figure 4. As for Figure 3, but for temperature fields.

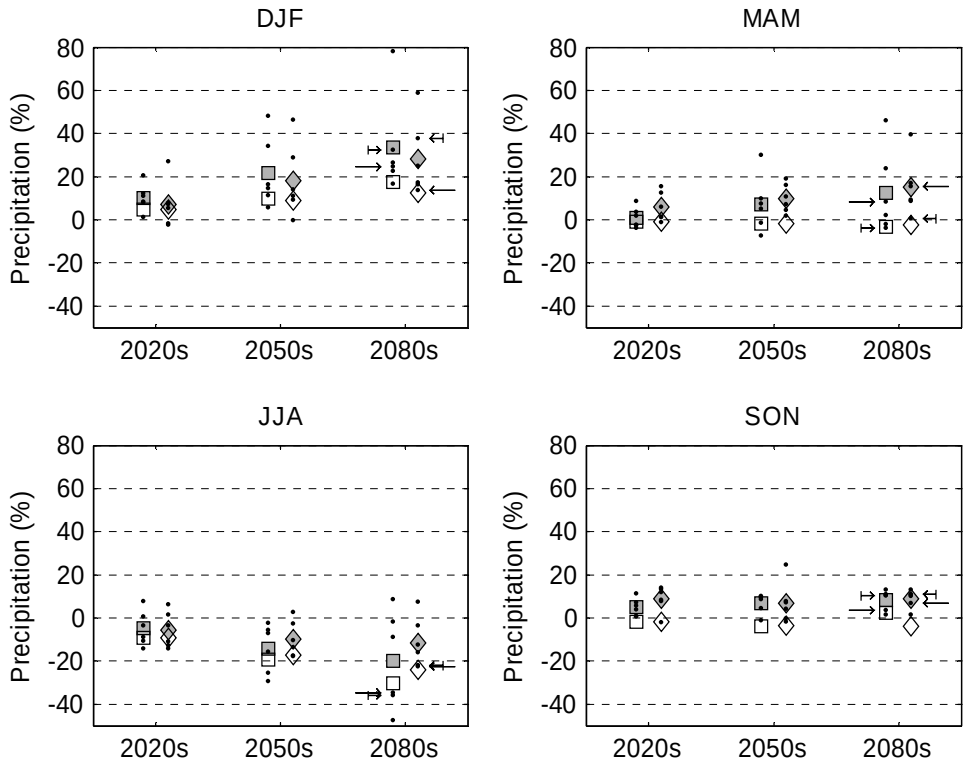

Figure 5. Projected changes for seasonal mean precipitation averaged over the UK, in percent of observed baseline climate. Points represent changes from individual GCMs and for three thirty-year periods. For each period, projected changes contain two groups of points at different locations on the x-axis representing A2 (left) and B2 (right) emissions scenarios. Grey filled squares and diamonds show multi-model ensemble means, respectively under the A2 and B2 scenarios. White squares and diamonds indicate corresponding UKCIP02 means. For comparison with previous studies, long arrows indicate HadCM3 ensemble member changes, and short arrows in winter and summer panels indicate ECHAM4 ensemble member changes (see text for details).

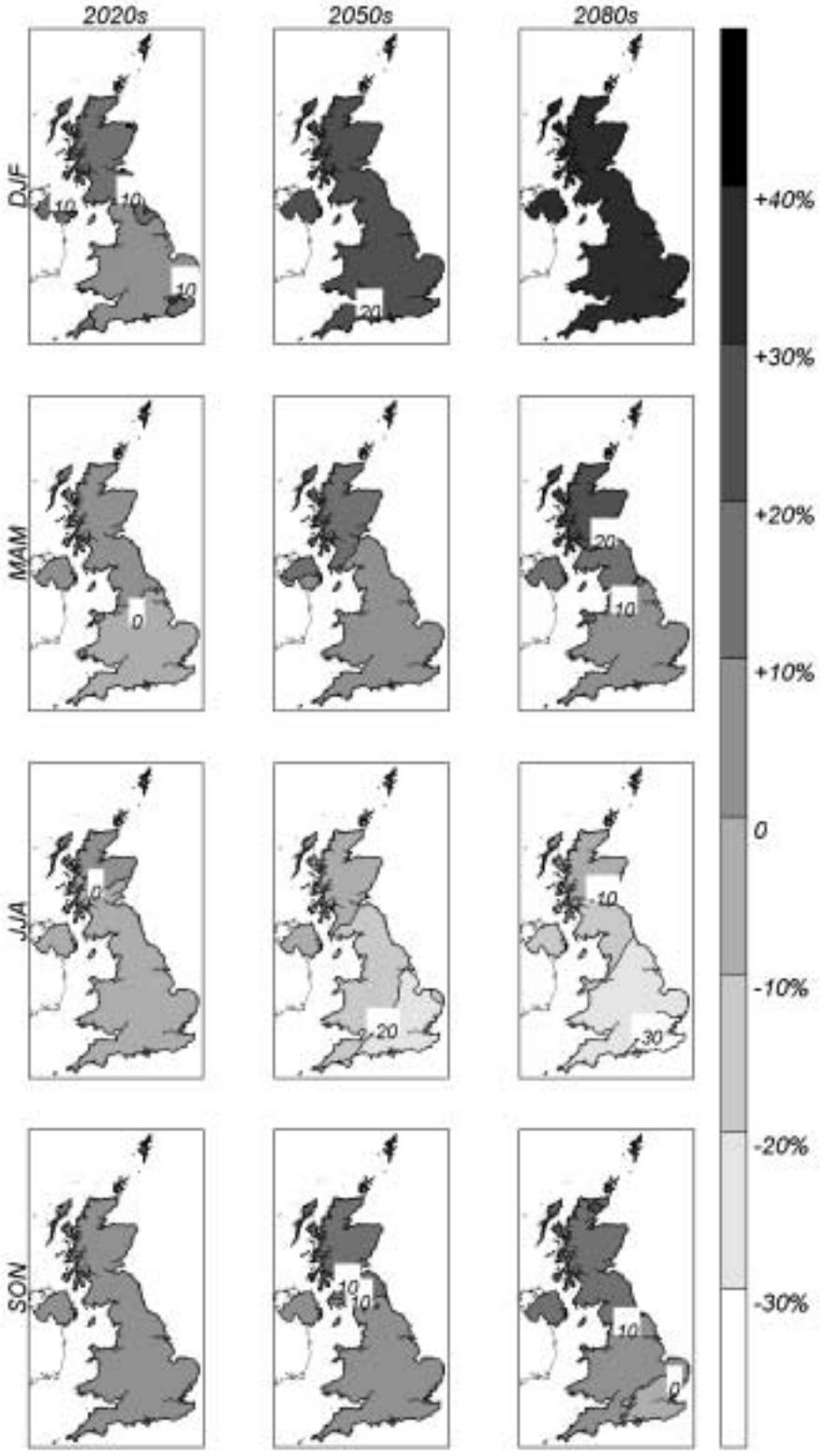
2020s
2050s
2080s
DJF
MAM
JJA
SON
+40%
+30%
+20%
+10%
0
-10%
-20%
-30%

Figure 6. Ensemble seasonal mean precipitation changes for the UK under the A2 emissions scenario. Changes are given in percent of the observed baseline means.

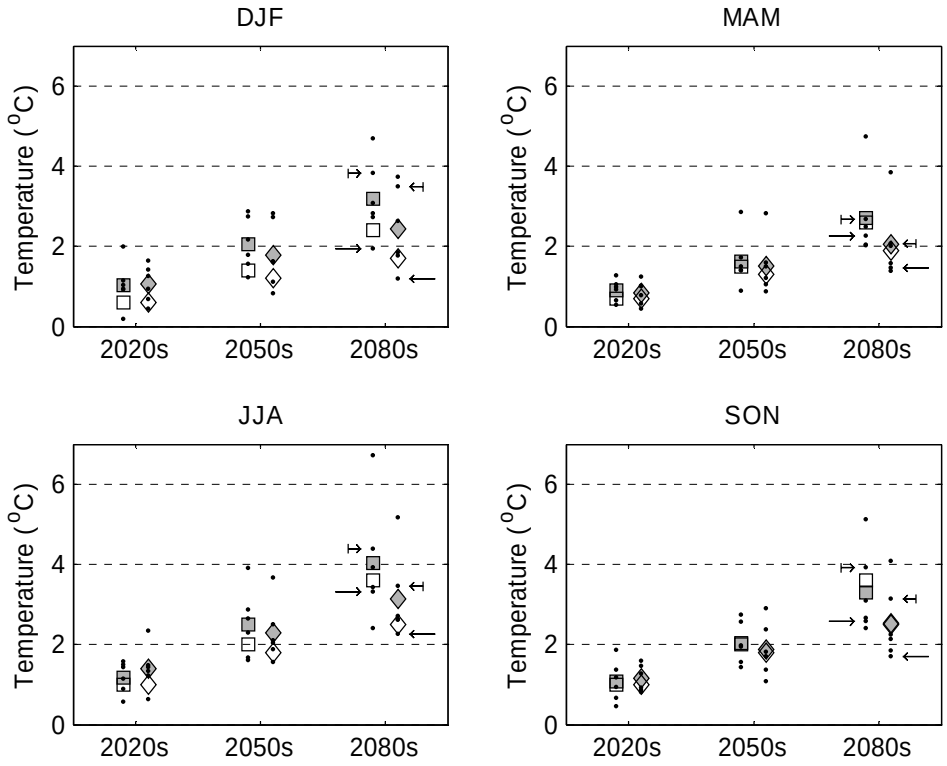

Figure 7. As for Figure 5, but for temperature. Changes are given as differences in degrees Centigrade from observed baseline climate.

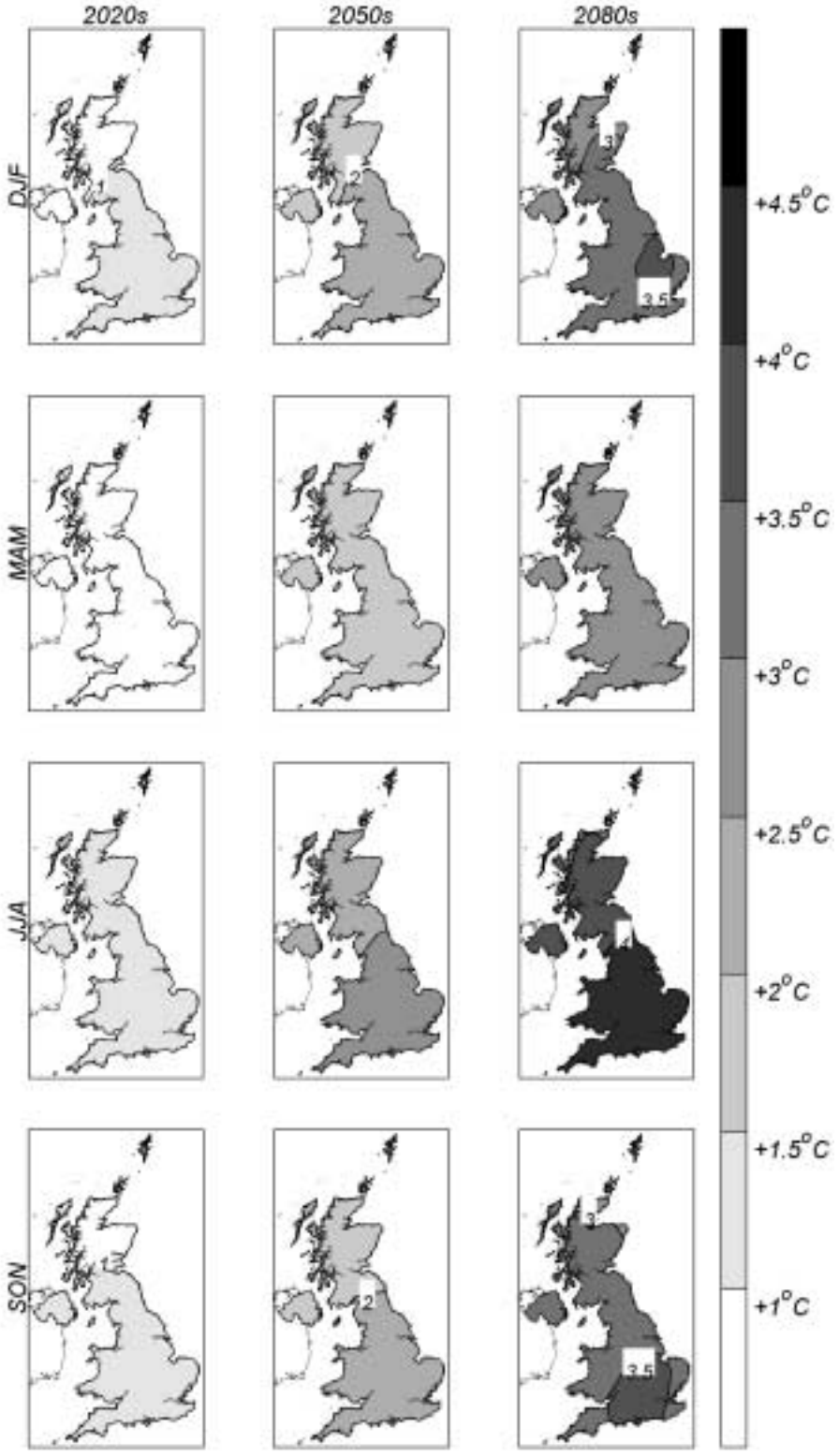
2020s
2050s
2080s
DJF
MAM
JJA
SON
1
2
3
3.5
4
+4.5°C
+4°C
+3.5°C
+3°C
+2.5°C
+2°C
+1.5°C
+1°C

Figure 8. As for Figure 6, but for temperature. Changes are given as absolute difference in degrees centigrade from the observed baseline means.

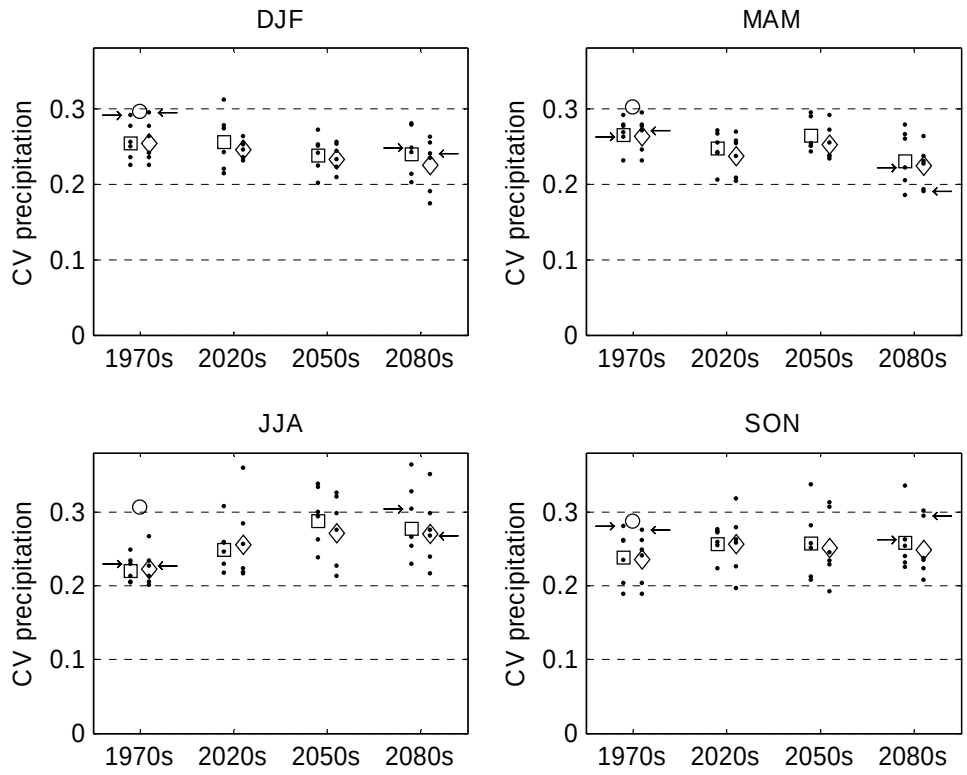

Figure 9. Precipitation interannual variability averaged over the UK, computed as thirty-year period coefficient of variation. Results are shown for the baseline period and for the three target periods. Points represent results from individual ensemble members. For each period, two groups of points are shown at different locations on the x-axis representing A2 (left) and B2 (right) scenarios. Squares and diamonds show multi-model ensemble values, respectively under the A2 and B2 scenarios. White circle represent observed baseline interannual variability. For comparison with previous studies, arrows indicate HadCM3-em values for the baseline period and for the 2080s (see text for details).

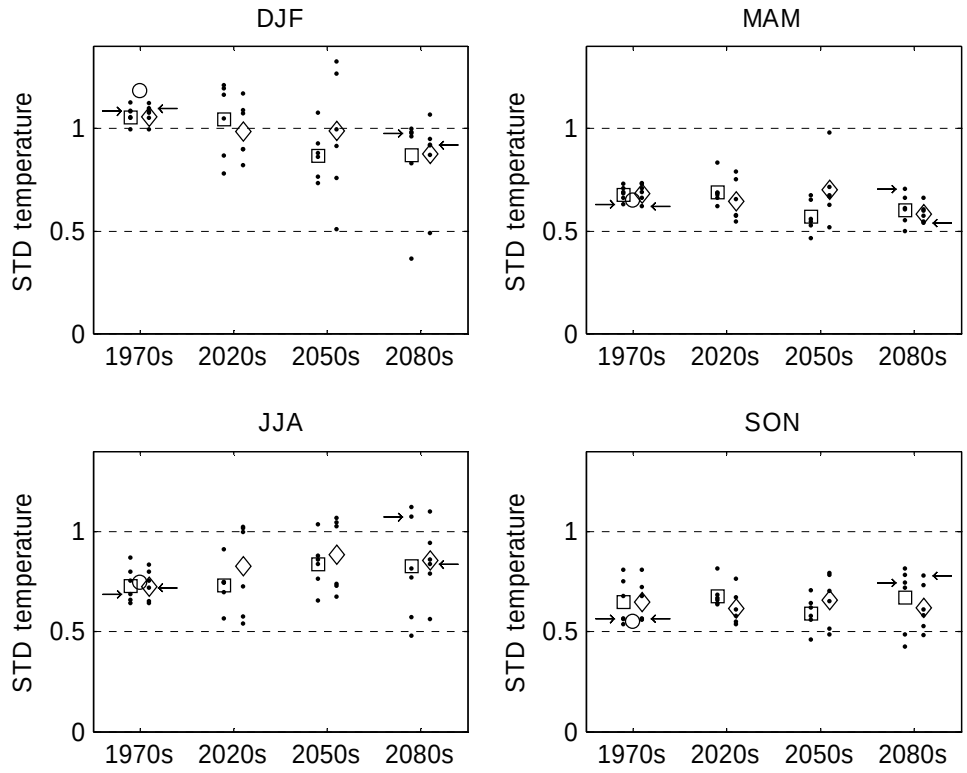

Figure 10. Temperature interannual variability averaged over the UK, computed as thirty-year periods standard deviation. Notations are the same as for Figure 9.